Effect of aging time on the availability of freshly precipitated ferric hydroxide to coastal marine diatoms

Masahiko Yoshida[1], Kenshi Kuma[1, 2]*, Shouei Iwade[1], Yutaka Isoda[1], Hyoe Takata[1] and Masumi Yamada[2]

[1]Graduate School of Fisheries Sciences, Hokkaido University, Hakodate, Hokkaido 041-8611, Japan

[2]Graduate School of Environmental Science, Hokkaido University, North 13 West 8, Kita-Ku, Sapporo, Hokkaido 060-0813, Japan

*Corresponding author: Kenshi Kuma, Graduate School of Fisheries Sciences, Graduate School of Environmental Science, Hokkaido University, North 13 West 8, Kita-Ku, Sapporo, Hokkaido 060-0813, Japan
Tel & Fax: +81-11-706-5314
E-mail: kuma@fish.hokudai.ac.jp

KEY WORDS: Iron uptake · Growth rate · Ferric hydroxide· Dissolution rate · Coastal marine diatom · *Chaetoceros sociale* · *Thalassiosira weissflogii*

Running title: Bioavailability of ferric hydroxide to marine diatoms

Abstract

Cell growth and iron uptake of the coastal marine diatoms, *Chaetoceros sociale* and *Thalassiosira weissflogii*, in the presence of short-aged amorphous ferric hydroxide (am-Fe(III)) media, which were prepared by aging for 1 d, 3 d and 3 weeks after adding a small amount of ferric iron acidic stock solution to autoclaved filtered seawater, were experimentally measured in culture experiments at 10°C for *C. sociale* and 20°C for *T. weissflogii*. The order of cell yields for both species was: 1-d aged am-Fe(III) > 3-d aged am-Fe(III) >> 3-weeks aged am-Fe(III) media. The iron uptake rates by *C. sociale* during 0–1 d in 1-d and 3-d aged am-Fe(III) media were about two-third and one-fourth, respectively, lower than that in the direct Fe(III) input medium containing *C. sociale* into which an acidic Fe(III) stock solution was added directly. The longer aging time of am-Fe(III) in media results in reducing the supply of bioavailable iron in media by the slower dissolution rate of am-Fe(III) with the longer aging time. These results suggest that the chemical and structural changes of freshly precipitated amorphous ferric hydroxide with short aging time affect their ability, such as iron solubility and dissolution rate, to supply bioavailable iron for the phytoplankton growth. The chemical and structural conversion of solid iron phases with time is one of the most important processes in changing the supply of available iron to marine phytoplankton in estuarine and coastal waters and in iron fertilization experiments.

Introduction

Iron is an essential micronutrient for phytoplankton growth, as an important component of such biochemical processes as photosynthetic and respiratory electron transport, nitrate and nitrite reduction, and a number of other biochemical reactions (Weinberg 1989; Geider and Roche 1994). Acquisition of iron by phytoplankton occurs through a complex series of extracellular reactions that are influenced by iron chemistry and speciation in seawater. In oxic seawater, iron is present predominantly in the insoluble (extremely low solubility) and thermodynamically stable 3+ oxidation state (Morel and Hering 1993; Stumm and Morgan 1996; Waite 2001). The inorganic speciation of Fe(III) in seawater is dominated by its hydrolysis behavior and ready tendency to precipitate to particulate Fe(III) hydroxide. Recent studies of the Fe(III) hydroxide solubility in seawater suggest that the Fe(III) solubility is controlled by organic complexation (Kuma et al. 1996; Waite 2001; Liu and Millero 2002; Tani et al. 2003; Chen et al. 2004; Takata et al. 2004, 2005), which, subsequently, regulates dissolved iron concentrations in seawater (Johnson et al. 1997a, b; Archer and Johnson 2000; Nakabayashi et al. 2001; Kuma et al. 2003; Rose and Waite 2004). There is also a strong temperature effect here with high solubility at low temperatures (Liu and Millero 2002). In a previous study (Kuma et al. 1996), the iron solubility limit of fresh solid amorphous $Fe(OH)_3$ in ultraviolet (UV)-irradiated open-ocean waters (free of organic ligands) was 0.07–0.09 nmol L^{-1} ($\leq$0.1 nmol L^{-1}). In addition, Wu et al. (2001) also reported that the iron solubility limit for inorganic Fe(III) hydrolysis species (Fe(III)') in the UV-irradiated seawater was ~0.08±0.03 nmol L^{-1}. Therefore, the equilibrium concentration of ~0.1 nmol L^{-1} only applies for iron in equilibrium with a fresh amorphous solid $Fe(OH)_3$ and is a maximum limit on Fe(III)' in seawater.

In general, the iron uptake rate by phytoplankton is primarily a function of the equilibrium concentration of Fe^{3+} in seawater and is actually dependent on the concentration of dissolved inorganic Fe(III) species ([Fe(III)']), which is proportional to [Fe^{3+}] (Free-ion activity model (FIAM)) (Anderson and Morel 1982; Hudson and Morel 1990; Campbell 1995; Sunda 2001), although apparent exceptions to the FIAM exist: for example, specific transport ligands such as siderophores that may be directly or indirectly utilized by cells (Maldonado and Price 2000, 2001; Sunda 2001). Therefore, the iron uptake of phytoplankton is limited by the equilibrium concentration of Fe(III)'

with particulate Fe(III) hydroxide and the slow dissolution rate of particulate Fe(III) in seawater if the dissolution rate of particulate Fe(III) is slow in relation to the further demands of the phytoplankton. Phytoplankton growth is probably controlled by the solubility and the dissolution rate of particulate Fe(III) hydroxide. In the previous studies (Kuma et al. 1999, 2000), it has been suggested that the natural organic Fe(III) complexes, such as fulvic-Fe(III) complex, and acidic Fe(III) supplied by riverine and eolian inputs play an important role in supplying bioavailable Fe(III)', above the equilibrium concentration of Fe(III)', in estuarine mixing systems and coastal waters through its dissociation and hydrolytic precipitation at high pH of seawater and high levels of seawater cations (Stumm and Morgan 1996). Recently, it has been reported that small colloidal Fe (<0.2 μm size) and Fe bound with natural colloids were biologically available depending on the colloidal geochemical characteristics (Nishioka and Takeda 2000; Chen and Wang 2001; Chen et al. 2003; Wang and Dei 2003). However, the crystalline ferric oxyhydroxides and ferric oxides, such as α-FeOOH (goethite), β-FeOOH (akaganeite) and α-Fe_2O_3 (hematite) did not support autotrophic phytoplankton growth at all (Wells et al. 1983; Rich and Morel 1990; Kuma and Matsunaga 1995). Therefore, the thermodynamic stability of iron colloids may be important in controlling the supply of bioavailable inorganic species of iron.

It is assumed that the chemical and structural changes of freshly precipitated amorphous ferric hydroxide (am-Fe(III)) with time and water temperature in estuarine and coastal waters affect their ability, such as iron solubility and dissolution rate of am-Fe(III), to supply bioavailable iron. In the present study, we examined that the chemical changes of freshly precipitated am-Fe(III) with aging time at 10 and 20°C will affect their ability to supply iron for the growth of coastal marine diatoms *Chaetoceros sociale* and *Thalassiosira weissflogii*. Solid am-Fe(III) forms used in our study are short-aged amorphous ferric hydroxide at 10 and 20°C, which were prepared by aging for 1 d, 3 d and 3 weeks after adding a small amount of ferric iron acidic stock solution to autoclaved filtered seawater (10°C for *C. sociale* and 20°C for *T. weissflogii*).

Materials and methods

In the present study, seawater was collected from a coastal region near

Hokkaido, Japan, in the northern Japan Sea (salinity= 33.8) and was filtered through an acid-cleaned 0.22-μm Millipore cellulosic membrane filter. The Fe concentration in the filtered seawater was determined by an automated Fe analyzer (Kimoto Electric) with use of a combination of chelating resin concentration and luminol-hydrogen peroxide chemiluminescence (CL) detection in a closed flow-through system (Obata et al. 1993, 1997) after the filtered seawater was buffered at pH 3.2 with a 10 mol L^{-1} formic acid–2.4 mol L^{-1} ammonium formate buffer solution (0.5 ml per 100-ml filtrate). The Fe concentration was ≤2 nmol L^{-1}. The concentrations of NO_3+NO_2, PO_4, and $Si(OH)_4$ in the filtered seawater measured by a Technicon autoanalyzer were less than 0.5, 0.1, and 5 μmol L^{-1}, respectively, which are negligible values compared with the concentrations added in the culture experiments (*see below*). Desferrioxamine B (DFB, sold commercially under the tradename Desferal), which is a strong Fe(III)-complexing agent forming a 1:1 DFB-Fe(III) complex, was purchased from Sigma Chemical as a fungal hydroxamate siderophore. The terrestrial fungal siderophore DFB is light sensitive and should be stored at less than 0°C. It has been found that addition of excess concentrations of the hydroxamate siderophore DFB essentially eliminated iron uptake in picoplankton-dominated community by diminishing the concentration of bioavailable Fe(III)' (Wells et al. 1994) and regulated iron availability in coastal upwelling waters (Wells 1999; Hutchins et al. 1999; Wells and Trick 2004). DFB is a small trihydroxamate molecule that specially complexes inorganic Fe(III) with an extremely high conditional stability constant ($K'_{FeL,Fe(III)}$=[Fe(III)L]/[Fe(III)'][L']=$10^{16.5}$ M^{-1}; Rue and Bruland 1995) in seawater (Hudson et al. 1992). In the present study, the growth with intracellular Fe stored by initial iron uptake of phytoplankton was measured by addition of hydroxamate siderophore DFB to prevent further iron uptake from ambient extracellular Fe in the media.

Culture experiments

All the preparation and sampling experiments were performed in a Class 100 laminar flow cabinet to avoid in advertent trace metal contamination. The polycarbonate bottles for the diatom culture and uptake experiments were first soaked in acid and rinsed with Milli-Q water (18.0 MΩ). The filtered seawater was autoclaved for 20 min

at 121°C (1.1 kg cm^{-2} pressure), and the culture medium was prepared by adding modified f/2 nutrient (Guillard and Ryther 1962) without trace metals and EDTA to the autoclaved filtered seawater. The modified f/2 medium contained 880 μmol L^{-1} nitrate, 38 μmol L^{-1} phosphate, and 105 μmol L^{-1} silicate. The large chain-forming coastal marine diatoms *C. sociale* and *T. weissflogii* were grown in 1 liter of the f/2 media at 10 and 20°C, respectively, to which ferric iron stock solution (25 μmol L^{-1} Fe(III); $FeNH_4(SO_4)_2 \cdot 12H_2O$ in 5 mmol L^{-1} HCl, pH 2.3) was added to make an iron concentration of 100 nmol L^{-1}. Cells were grown under 150 μmol photons m^{-2} s^{-1} fluorescent light (12 h light: 12 h dark) to obtain the cell concentration expected at the start of the following culture and iron uptake experiments.

Small amounts of ferric iron acidic stock solution and DFB solution were immediately mixed in a precleaned 100-ml polycarbonate Erlenmeyer flask. Desferrioxamine B medium was prepared by adding 50 ml of autoclaved filtered seawater at 10°C for *C. sociale* (cell diameter: ~6 μm, height: ~12 μm) and at 20°C for *T. weissflogii* (cell diameter: ~8 μm, height: ~13 μm) to premixed DFB-Fe(III) (10:1) solution in the flask to ensure which DFB:Fe(III) (10:1) inhibit the growth of *C. sociale* and *T. weissflogii* over at least 11–15 d in culture experiments. Solid amorphous ferric hydroxide (am-Fe(III)) media were prepared by aging for 1 d, 3 d and 3 weeks after adding a small amount of ferric iron acidic stock solution to 50 ml of autoclaved filtered seawater (10°C for *C. sociale* and 20°C for *T. weissflogii*). The final iron concentration was 100 nmol L^{-1}. An f/2 nutrient stock solution and then a small amount of culture (ca. 250 μl) in an initial stationary growth phase were added to each culture flask. All major nutrient stocks were passed through Chelex 100 ion-exchange resin to remove trace metals (Morel et al. 1979). The Fe concentration in the control culture medium (the autoclaved filtered seawater which nutrient was added) was ≤3.5 nM. The effect of direct Fe input was examined by adding a small amount of acidic ferric iron stock solution directly together with an inoculation of culture into the control culture media. In the previous study (Kuma et al. 2000), the high Fe(III)' concentration in direct Fe(III) input medium was remarkably bioavailable and induces the highest iron uptake and growth of coastal marine phytoplankton. In addition, the growth of phytoplankton by intracellular Fe were examined by addition of DFB to final concentration of 1 μmol L^{-1} (DFB:Fe(III)=10:1) after 1 d cultivation in direct Fe(III) input medium and in 1-d and 3-d aged am-Fe(III) media to prevent further iron uptake by phytoplankton from

ambient external Fe (dissolved Fe(III) and solid Fe(III) hydroxide in media). Moreover, *T. weissflogii* was grown in 1-d aged am-Fe(III) media and direct Fe(III) input media with iron concentrations of 10, 25 and 50 nmol L^{-1} in addition to 100 nmol L^{-1}. Control (without any added iron) media were prepared to compare the growth rates and cell yields with those containing iron. Cell concentrations at the start of the culture experiments were approximately 1,000 cells ml^{-1}. The light, temperature and nutrient conditions were the same as those of the stock culture described above. During the experiments, cell growth was monitored daily by triplicate cell counts done with an optical microscope. Culture experiments were conducted in triplicate.

Iron uptake experiments

Iron uptake experiments were conducted with *C. sociale* grown in direct Fe(III) input and 1-d and 3-d aged am-Fe(III) media which DFB was added just after 1 d cultivation. The long-term (daily for 1–7 d) iron uptake experiments were carried out in media to which $^{59}Fe(III)$ was added. Incubations were done at 10°C under 150 µmol photons m^{-2} s^{-1} fluorescent light (12 h light: 12 h dark).

The direct $^{59}Fe(III)$ input culture was prepared by adding a small amount of premixed solution of acidic stock radioactive $^{59}Fe(III)$ (New England Nuclear Corp., NEZ-037) solution (7 µmol L^{-1} Fe(III); $^{59}FeCl_3$ in HCl, pH ~2.2–2.3) and ferric iron acidic stock solution (25 µmol L^{-1} Fe(III), pH 2.3) to 1000 ml of autoclaved filtered seawater (10°C), which already contained modified f/2 nutrient and *C. sociale* culture in initial stationary growth phase. The pH of culture solution after premixed acidic radioactive $^{59}Fe(III)$ addition was 7.98–8.05.Solid aged am-$^{59}Fe(III)$ cultures were prepared by adding modified f/2 nutrient and *C. sociale* culture (approximately 50 ml), after adding premixed $^{59}Fe(III)$ solution to 950 ml of autoclaved filtered seawater (10°C) and then aging for 1 and 3 d at 10°C. *C. sociale* cell concentration at the start of the iron uptake experiments were ca. 10,000 cells ml^{-1}. The final iron concentration was 100 nmol L^{-1}. The nutrient concentrations were the same as those in the culture experiments described above.

At each sample point (daily for 1–7 d) during the long-term iron uptake experiment, a 50-ml aliquot was mixed with 20 ml of 0.175 mol L^{-1}

Ti(III)–citrate–EDTA solution (0.175 mol L^{-1} $TiCl_3$, $Na_3citrate{\cdot}2H_2O$, and $Na_2EDTA{\cdot}2H_2O$ in filtered seawater, followed by an adjustment of the pH to 8 with NaOH solution) as demonstrated by Hudson and Morel (1989, 1990). The Ti(III) solution was used to rapidly dissolve freshly precipitated am-Fe(III) and extracellularly adsorbed iron by reductive dissolution of Fe(III) without cellular damage to *C. sociale*. After the mixture was allowed to stand for 10 min, it was gently vacuum filtered through a quantitative filter paper (No. 5C, Advantec) that retains all precipitate ≥1 μm in size. The filter was rinsed with 30 ml of 0.05 mol L^{-1} Ti(III) solution which was prepared by diluting 0.175 mol L^{-1} Ti(III)–citrate–EDTA solution with filtered seawater. The drained filter was digested with 7 ml of conc. HNO_3 : conc. $HClO_4$ (1:1) and then diluted to 20 ml. The γ-activity of 4 ml of diluted sample in a counting vial was measured using a gamma counter (Aloka ARC-301B), and the results were converted to amounts and rates of iron incorporation. In addition, iron uptake experiments for cell-free control media (direct ^{59}Fe(III) and 1-d and 3-d aged am-^{59}Fe(III)) at 10°C were conducted to ascertain the reductive dissolution of freshly precipitated and aged am-Fe(III) by the Ti(III) solution. In previous studies (Kuma and Matsunaga 1995; Kuma et al. 2000), freshly precipitated am-Fe(III) (aged for less than 1 d at 10°C) was almost completely dissolved by the reductive dissolution with Ti(III) treatment. However, aged am-Fe(III) produced in direct Fe(III) input cell-free media during aging above 1 d at 10°C was incompletely reductively dissolved by Ti(III) solution in the present study and even by new oxalate reagent wash technique (Tovar-Sanchez et al. 2003) because of the much slower dissolution of aged am-Fe(III). The dissolution rates of am-Fe(III) phase decrease with aging time because of the slow conversion to more stable phases (Kuma and Matsunaga 1995). Therefore, iron uptake at each sample point during iron uptake experiments was determined by subtracting the amount of insoluble iron in cell-free medium from the amount of iron uptake in medium containing cells. During the experiments, cell growth at each culture was monitored by triplicate cell counts done with an optical microscope.

Hydrolytic precipitation of Fe(III) in seawater

Hydrolytic precipitation rate of Fe(III) in the 0.22-μm-filtered seawater was

measured at 10°C and 20°C by a simple filtration technique involving γ-activity measurement of ^{59}Fe previously reported by Kuma et al. (1996, 1998a, 1998b). To examine the effect of aging time and temperature (10 and 20°C) on hydrolytic precipitation of Fe(III) in seawater, a small amount of ^{59}Fe(III) stock solution, previously spiked with a small known amount of stable Fe(III), was added to 250 ml of the 0.22-μm–filtered seawater in acid-cleaned 250-ml Teflon bottles (10 and 20°C). The final iron concentration was 100 nmol L^{-1}. In general, the addition of dissolved inorganic Fe(III) to seawater results in rapid hydrolytic precipitation of metastable Fe(III) hydroxide, which slowly converts to more stable solid phases (Kuma and Matsunaga 1995; Stumm and Morgan 1996). The bottles containing the seawater solution and radiolabelled Fe(III) were kept in an incubator (dark condition) at 10 and 20°C. During standing in the dark for 3 weeks at 10 and 20°C, each 7.5-ml sample aliquot was filtered through a 0.025-μm Millipore cellulosic membrane filter and acidified by addition of 10 μl of concentrated HCl to prevent adsorption of filtered Fe(III) on the wall of the collecting vial. The γ-activity of the 2.5-ml acidified sample filtrates were measured in 5-ml counting vials with a gamma counter. Finally, the 0.025-μm-filtered Fe(III) concentrations (Fe(III) hydroxide solubility) were calculated from the γ-activity (Kuma et al.1996, 1998a).

Results

Growth rate and cell yields for *C. sociale* and *T. weissflogii*

Fig. 1 presents the results of the culture experiments for *C. sociale* (10°C) and *T. weissflogii* (20°C) in direct Fe(III) input and DFB-Fe(III) (10:1) media. In the present study, direct Fe(III) input to the culture solution induced the highest growth rate and the highest maximal cell yields (0.52 d^{-1} and 150,000 cells ml^{-1} for *C. sociale* and 0.63–0.64 d^{-1} and 170,000 cells ml^{-1} for *T. weissflogii*, respectively, Table 1), similar value to that in the same medium for *C. sociale* in the previous study (Kuma et al. 2000). However, there was no growth in DFB-Fe(III) (10:1) medium for both species. Therefore, the effect of direct Fe(III) input, aging time of particulate am-Fe(III) and the growth by intracellularly stored Fe were examined by addition of DFB (final

concentration of 1 μmol L^{-1} (DFB:Fe(III)=10:1)) during cultivation to prevent iron uptake from ambient extracellular Fe. Desferrioxamine B was added to *C. sociale* and *T. weissflogii* cultivated for 1 d in direct Fe(III) input medium (direct Fe(III)-DFB) and 1-d and 3-d aged am-Fe(III) media (1-d aged am-Fe(III)-DFB; 3-d aged am-Fe(III)-DFB).

For the culture experiment of *C. sociale* without any addition of DFB, the relative order for maximal cell yields on different media for 8–12 days cultivation was direct Fe(III) input > 1-d aged am-Fe(III) > 3-d aged am-Fe(III) >> 3-weeks aged am-Fe(III) > control (no iron) although the initial growth rates in all media except for control were almost same with 0.45–0.53 d^{-1} (Fig. 2a, Table 1). These results then suggest that the time history of exposure to iron is very important in assessing the growth rate. The growth in direct Fe(III)-DFB, 1-d aged am-Fe(III)-DFB and 3-d aged am-Fe(III)-DFB media (Fig. 2b) continued for 5–8 d even after addition of DFB with almost same maximum growth rate (~0.42–0.49 d^{-1}) as those in all Fe(III) media without any addition of DFB (Table 1). Cell concentration in the direct Fe(III)-DFB medium increased up to approximately 40,000 cells ml^{-1}, 40 times more than initial cell concentration, by 8 d cultivation after addition of DFB. The relative order for maximal cell yields was direct Fe(III)-DFB > 1-d aged am-Fe(III)-DFB > 3-d aged am-Fe(III)-DFB media, while the initial growth rates were almost the same in all media (Fig. 2b).

For the culture experiment of *T. weissflogii*, the maximal cell yields and the growth rates were the same in all media, except for 3-w aged am-Fe(III) and control media, without any addition of DFB (Fig. 3a, Table 1). However, the growth in direct Fe(III)-DFB, 1-d aged am-Fe(III)-DFB and 3-d aged am-Fe(III)-DFB media continued for 4–5 d even after addition of DFB with the almost same maximum growth rate (~0.57–0.61 d^{-1}) as those in all Fe(III) media without addition of DFB but with different maximal cell yields (Fig. 3b, Table 1). The similar maximal growth rates but different cell yields suggest that the length of the exponential growth phase differed between the iron treatments. The order of maximal cell yields after addition of DFB was direct Fe(III)-DFB > 1-d aged am-Fe(III)-DFB > 3-d aged am-Fe(III)-DFB media, the same order as that for *C. sociale* (Table 1). The maximal cell yields in direct Fe(III) input media with lower iron concentrations (10, 25 and 50 nmol L^{-1}) than 100 nmol L^{-1} were higher than those in 1-d aged am-Fe(III) media with same iron concentrations (Fig. 3c, Table 1) although the maximal cell yields and the growth rates were the same in direct

Fe(III) input, 1-d aged am-Fe(III) and 3-d aged am-Fe(III) media with iron concentration of 100 nmol L^{-1} (Fig. 3a).

Iron uptake and growth rate of *C. sociale*

The long-term iron uptake rates by *C. sociale* and the growth in direct Fe(III) input medium and 1-d and 3-d aged am-Fe(III) media, into which DFB were added after 1 d cultivation, were measured during cultivation for 7 d at 10°C (Fig. 4). The cellular iron uptake (nmol L^{-1}) by *C. sociale* in all media was prevented by addition of DFB and remained nearly constant for 4 d after DFB treatment (Fig. 4a). However, the iron uptakes after 5 d decreased gradually with decreasing in cell concentrations during 5–7 d. The iron uptake rate during 0–1 d in 3-d aged am-Fe(III) medium was approximately one-fourth lower than that in direct Fe(III) input medium and two-fifth lower than that in 1-d aged am-Fe(III) medium. The order of mean iron uptake for 4 d after addition of DFB was direct Fe(III)-DFB > 1-d aged am-Fe(III)-DFB > 3-d aged am-Fe(III)-DFB (Fig. 4a, Table 2).

Cell concentrations in media, which were prevented from further iron uptake from ambient extracellular Fe by addition of DFB, increased logarithmically for 1–2 d even after addition of DFB (Fig. 4b). The initial growth rates (0.44±0.04–0.47±0.01 d^{-1}) in DFB-added media were nearly the same as those (0.42–0.53 d^{-1}) in all media with and without addition of DFB (Table 1). However, the maximal cell yields in DFB-added media were one-fourth to one-half lower than that in direct Fe(III) input medium without any addition of DFB. The order of maximal cell yields was: direct Fe(III) input (no DFB) > direct Fe(III)-DFB > 1-d aged am-Fe(III)-DFB > 3-d aged am-Fe(III)-DFB.

Hydrolytic precipitation of Fe(III) at 10 and 20°C

Figure 5 presents the results of the Fe(III) hydrolytic precipitation rates of Fe^{3+} in filtered seawater at 10 and 20°C. The hydrolytic precipitation rates of Fe^{3+} in filtered seawater were extremely fast, resulting in extremely low 0.025 μm filterable (dissolved) Fe concentrations within short aging times. For example, the dissolved Fe

concentrations with 1 d aging were 6.2 and 1.9 nmol L^{-1} at 10 and 20°C, respectively. The dissolved Fe would include small colloidal and soluble Fe species and the colloidal species may be removed rapidly through particle/particle interactions (Honeyman and Santschi 1991). In addition, the hydrolytic precipitation rate of Fe^{3+} at 10°C was slower than that at 20°C. The dissolved Fe concentrations at 10°C decreased gradually 1.98 to 0.74 nmol L^{-1} during aging for 1 to 3 weeks, while those at 20°C were nearly constant within the range 0.26 to 0.36 nmol L^{-1} during 1–3 weeks. The long term dissolved (soluble) iron concentrations of ~0.3 nmol L^{-1} are most likely due to the presence of soluble iron organic species as mentioned above.

Discussion

Effect of aging time on bioavailability of freshly precipitated ferric hydroxide

Direct Fe(III) input medium promoted the maximal cell yields and growth rate (Fig. 1). However, there was no growth in premixed DFB-Fe(III) complex (10:1) media. In general, iron uptake rate by marine eukaryotic phytoplankton is related to the concentration of kinetically labile inorganic Fe species ([Fe']: [Fe(II)'] and [Fe(III)']), which is proportional to $[Fe^{2+}]$ and $[Fe^{3+}]$, respectively, and independent of the concentration of Fe chelated to organic ligands such as EDTA and DFB (Campbell 1995, Sunda 2001) although the iron uptake rates from DFB-Fe complex by iron-limited phytoplankton are more correlated to the concentrations of DFB-Fe complex than those of Fe' (Maldonado and Price 2000, 2001). The equilibrium calculation in premixed DFB-Fe(III) (10:1; Fe(III)=100 nmol L^{-1}) medium indicates that bioavailable Fe(III)' would be limited to ~10^{-17} mol L^{-1} ($K'_{FeL,Fe(III)'}$ =$10^{16.5}$ M^{-1}, Rue and Bruland 1995, Croot and Johansson 2000), or several orders of magnitude below the levels needed to support phytoplankton growth. In the present study, the direct input of Fe(III) into the culture media containing phytoplankton induced the highest radiolabelled iron uptake rate ($[D_{radio}]/[C_{DFB}]$ = ~3x10^{-16} mol $cell^{-1}$ d^{-1}, Table 2) by *C. sociale* during the first day of incubation in the long-term iron uptake experiment (Fig. 4a), resulting from the high supply of bioavailable Fe(III)'. In addition, the highest iron uptake rate (~3x10^{-17} mol $cell^{-1}$ h^{-1}) were also observed at short-term iron uptake experiment in the direct Fe(III)

input medium in our previous study (Kuma et al. 2000). Extremely high concentration of Fe(III)' represents the actual instantaneous availability of iron for uptake. Therefore, the direct input of concentrated acidic Fe(III) stock solution into culture media enhances the concentration of bioavailable Fe(III)' above the equilibrium concentration with solid amorphous Fe(III) hydroxide in seawater and induces the highest iron uptake rate and highest cell yields of phytoplankton (Figs 2, 3 and 4).

The stable oxidation state of iron in oxic seawater is Fe(III), which has an extremely low solubility and the hydrolytic precipitation rate of Fe^{3+} in seawater was extremely fast (Fig. 5). The equilibrium concentration of Fe(III)' with particulate Fe(III) hydroxide in seawater is approximately 0.1 nmol L^{-1} (Kuma et al. 1996, Wu et al. 2001), which limits the iron uptake of phytoplankton if the dissolution rate of particulate Fe(III) is slow in relation to the further demands of the phytoplankton. For the culture experiment of *C. sociale*, the longer aging time in solid am-Fe(III) media tends to be the lower maximal cell yields with a order of direct Fe(III) input > 1-d aged am-Fe(III) > 3-d aged am-Fe(III) > 3-w aged am-Fe(III) media with the same initial growth rates (Fig. 2a, Table 1). In addition, the relative order for maximal cell yields in media (direct Fe(III)-DFB > 1-d aged am-Fe(III)-DFB > 3-d aged am-Fe(III)-DFB) by addition of DFB after 1 d cultivation was the same as that for media without any addition of DFB (Fig. 2b, Table 1). However, there is no difference among direct Fe(III) input, 1-d aged Fe(III) and 3-d am-Fe(III) media with iron concentration of 100 nmol L^{-1} for the maximal cell yields and growth rates of *T. weissflogii* (Fig. 3a) although the lower maximal cell yields in solid am-Fe(III) media than direct Fe(III) medium were clearly observed in the culture experiments with addition of DFB after 1 d cultivation (Fig. 3b) and with lower iron concentrations such as 10, 25 and 50 nmol L^{-1} (Fig. 3c). It is likely that the dissolution rate of particulate Fe(III) with 100 nmol L^{-1} in culture media is sufficiently fast to accomplish the maximal cell yields and highest growth rate of *T. weissflogii,* Therefore, the lower concentration and the longer aging time of particulate Fe(III) in media result in the slower dissolution rate of particulate Fe(III), reducing the supply of bioavailable Fe(III)' in media.

Growth by intracellularly stored Fe for *C. sociale*

In the present study, the highest specific growth rates of *C. sociale* and *T. weisflogii* were maintained for 2–7 d even after addition of DFB, which prevented further iron uptake from ambient extracellular Fe in culture media (Figs 2b, 3b, 4b). The growth rate of *C. sociale* was independent of the amount of intracellularly stored Fe (Fig. 4, Table 1, 2). If cells are under identical steady state growth conditions both before and after addition of radiolabelled Fe, it is necessary to allow the phytoplankton to go through 8 successive transfers in order to measure intracellular Fe quotas by radioactive ^{59}Fe uptake, so that all the Fe within the cells is in isotopic equilibrium with the ^{59}Fe. The initial cultures in the iron uptake experiments had a cell density of 10,000 cells ml^{-1}. The growth rate was approximately 1 division per day (Fig. 4b). Thus, after 1 day, the cells density will increase to 20,000 cells ml^{-1} and cells will be 50% radiolabelled. In the next cell division, the Fe within the cells will be 75% radiolabelled and the cell density will reach 40,000 cells ml^{-1}. Therefore, if the cells are collected before undergoing 8 divisions, the intracellular Fe concentrations, which were measured with radioactive Fe, need to be corrected for the non-radioactive (cold) Fe in the cells at the beginning of the experiment. The corrected intracellularly stored Fe (Fe quota [Q]; mol Fe cell^{-1}) was calculated by dividing the amount of radiolabelled Fe uptake ([D_{radio}]: mol Fe ml^{-1}) for 1 d by cell density ([C_{DFB}]: cells ml^{-1}) when DFB was added for the Fe uptake measurements and percentage of intracellular radiolabelled Fe ([P]: %) (Fig. 4, Table 2):

$$[Q]=[D_{radio}]/[C_{DFB}]/[P]/100 \quad (1)$$

Values of corrected Fe uptake ([D_{radio}]/[P]/100) and Fe quota [Q] for the direct Fe(III) input medium (DFB (1 d)) and 1-d and 3-d aged am-Fe(III) media (DFB (1 d)) are also the iron uptake rates with units of mol Fe ml^{-1} d^{-1} and mol Fe cell^{-1} d^{-1}, respectively (Table 2). The corrected cellular Fe [Q] in culture media ranged 3.1–9.8x10^{-16} mol Fe cell^{-1} and the highest value was found in the direct Fe(III) input medium (DFB (1 d)) (Table 2). However, the maximal cell yields ([Cn]; cells ml^{-1}) appeared to be relatively dependent on the amount of intracellular Fe, suggesting the presence of a critical concentration of intracellular Fe (minimum cellular Fe on growth) on phytoplankton growth (Fig. 4). The critical intracellular Fe ([Q_{cri}]: mol Fe cell^{-1}) is calculated by multiplying [Q] by [C_{DFB}] and then by dividing by [Cn] (Table 2):

$$[Q_{cri}]=[Q]\cdot[C_{DFB}]/[Cn] \quad (2)$$

by assuming that 1) the cells reached stationary phase because of low Fe availability, and not because of either N, P, or Si became limiting, and 2) the Fe uptake was corrected for the additional cold Fe in the cells before the Fe uptake rate measurements were made. However, the iron uptake experiments in the present study were started with Fe-limited cells, which are documented to have higher iron uptake rates than Fe replete cells (Sunda & Huntsman 1995), under the excessive Fe(III)' conditions. Thus, after 1 day, the parameter [*P*] would be nearly 100% rather than 50%. Therefore, the value of [*Q*] was simply calculated by dividing the amount of radiolabelled Fe uptake ([D_{radio}]) for 1 d by cell density ([C_{DFB}]) when DFB was added for the Fe uptake measurements (Fig. 4, Table 2). Values of [D_{radio}] and [*Q*] are also the iron uptake rates with units of mol Fe ml^{-1} d^{-1} and mol Fe $cell^{-1}$ d^{-1}, respectively. Figure 6 presents a plot of the daily intracellular Fe per cell in direct Fe(III)-DFB, 1-d aged am-Fe(III)-DFB and 3-d aged am-Fe(III)-DFB media after addition of DFB. The daily intracellular Fe values in direct Fe(III)-DFB and 1-d aged am-Fe(III)-DFB media tend to be nearly constant (~$1x10^{-16}$ mol Fe $cell^{-1}$) after 3 d, probably indicating the critical cellular Fe. The highest intracellular Fe ([*Q*]= ~$3.4x10^{-16}$ mol Fe $cell^{-1}$, Fig. 6, Table 2) of *C. sociale* in the present study was approximately one-half lower than the Fe quota values ([*Q*]=~5–$9x10^{-16}$ mol Fe $cell^{-1}$) of *T. weissflogii* in the Fe sufficient media reported by Sunda & Huntsman (1995) and Maldonado & Price (1996). The critical concentration of intracellular Fe ([Q_{cri}]) on phytoplankton growth was simply calculated by dividing [D_{radio}] by [*Cn*] (minimum cellular Fe on growth: [Q_{cri}]=[D_{radio}]/[*Cn*]=[*Q*]x[C_{DFB}]/[*Cn*]= ~0.5–$1x10^{-16}$ mol Fe $cell^{-1}$ for *C. sociale*, Table 2). The critical cellular Fe values are also one-half lower than the Fe quota values (~0.7–$2x10^{-16}$ mol Fe $cell^{-1}$) for *T. weissflogii* in the Fe deficient media (Hudson & Morel 1990; Sunda & Huntsman 1995; Maldonado & Price 1996). The lower values of [*Q*] and [*Qcri*] for *C. sociale* are probably due to one-half smaller cell volume of *C. sociale* than *T. weissflogii.* However, values of [*Q*] and [Q_{cri}] for 3-d aged am-Fe(III) medium were unreliable because of low iron uptake and incomplete dissolution of aged am-Fe(III) by Ti(III) treatment (Kuma and Matsunaga 1995; Kuma et al. 2000). The Ti(III) solution (Hudson and Morel 1989, 1990) and the oxalate reagent (Tovar-Sanchez et al. 2003) treatments may overestimate

the intracellular Fe in field samples where aged amorphous ferric hydroxide and crystalline ferric oxyhydroxides may be present.

At high iron concentrations, phytoplankton can often accumulate an excess of iron than that needed to support maximum growth. Such luxury uptake at high iron concentrations was observed in a culture experiment of oceanic and coastal eukaryotic algae (Sunda and Huntsman 1995, 1997; Sunda 2001). We will discuss the luxury iron uptake elsewhere with supporting data by additional culture experiments. In the present study, the highest iron uptake by *C. sociale* was observed during the first day of incubation in the direct Fe(III) input medium and was 1.5 to 4 times higher than those in 1-d and 3-d aged am-Fe(III) media, respectively (Fig. 4a). The iron uptake rate by eukaryotic phytoplankton is generally dependent on the concentration of dissolved Fe(III)' (Anderson & Morel 1982; Campbell 1995). In solid am-Fe(III) media, therefore, the higher iron uptake rate by phytoplankton would have been accomplished by the shorter aged precipitated amorphous ferric oxide with the higher Fe(III)' dissolution rate because of the larger surface area. The Fe(III)' dissolution rate of amorphous phase decrease rapidly with aging time because of the conversion to more stable phases (Crosby et al. 1983; Wells et al. 1983, 1991; Kuma and Matsunaga 1995).

Conversion to more stable am-Fe(III) phases with less bioavailability

The hydrolytic precipitation rate of Fe^{3+} in seawater was fast, resulting in an extremely low 0.025-μm filterable (dissolved) Fe concentration with short aging time (Fig. 5). In general, the freshly precipitated am-Fe(III), in which very fine particles with a large surface area and structural disorder occur, consists of aggregates of hydrated ferric ions that have a very low thermodynamic stability. Freshly precipitated am-Fe(III) in solution undergoes continuous chemical changes with time (loss of water and increased crystallization) that are not easily quantified. An increase in the thermodynamic stability of am-Fe(III) substantially decrease the solubility and lability of the solid am-Fe(III) phase and thereby decrease iron availability to phytoplankton (Wells et al. 1983, 1991; Rich and Morel 1990; Kuma and Matsunaga 1995). In addition, it has been reported that small colloidal iron particle fraction (< 0.2 μm size) was the most dynamic size fraction during the growth of the diatom *Chaetoceros* sp. in

laboratory culture experiments (Nishioka and Takeda 2000). The actual particulate solid ferric hydroxide, oxyhydroxide, or oxide phase regulates the solubility of dissolved inorganic Fe species [Fe(III)'] and its influence on biological availability of iron. In the present study, the solubility measurements of am-Fe(III) in seawater indicated a rapid decrease of dissolved Fe concentrations with aging time (Fig. 5), suggesting that am-Fe(III) in seawater solution changes to larger and more stable particles with aging time (Crosby et al. 1983; Pankow 1991). In addition, lower temperature retarded the conversion to larger particles. In a previous study (Kuma and Matsunaga, 1995), proton-promoted dissolution rates of am-Fe(III) decreased rapidly with aging time. These above results suggest that the bioavailability of am-Fe(III) produced in culture solution decreases rapidly with time during culture experiments, resulting from a decreased dissolution rate of am-Fe(III) with time.

To interpret the temporal decrease in dissolved Fe concentrations with aging time in the Fe(III) hydrolytic precipitation experiment at 10°C (Fig. 5), we present a model assuming a first-order transfer reaction with a rate constant, k_1, from dissolved Fe to particulate Fe at an early period of rapid Fe(III) hydrolytic precipitation and a back reaction with a rate constant, k_2, from unstable fine particulate Fe to dissolved Fe in the slow conversion process to more stable particulate Fe with time. Here, a time-developing model between dissolved Fe and particulate Fe concentrations is given by

$$dD_{Fe}/dt = -k_1 D_{Fe} + k_2 P_{Fe} \quad (3)$$

$$dP_{Fe}/dt = k_1 D_{Fe} - k_2 P_{Fe} \quad (4)$$

where D_{Fe} and P_{Fe} are dissolved Fe and particulate Fe concentrations, respectively. We can roughly estimate k_1 =30 d^{-1} from a rapid decrease in dissolved Fe concentration at an early stage (less than 3 h) of Fe(III) hydrolytic precipitation experiments (Fig. 5) because of a first-order reaction of hydrolytic precipitation at $k_1 D_{Fe} >> k_2 P_{Fe}$. The initial values of D_{Fe} and P_{Fe} at $t=0$ are 100 and 0 nmol L^{-1}, respectively. In our model, however, a back reaction rate constant (k_2) is the unknown parameter so that the following three types of k_2 were considered as follows:

(i) Constant value: $k_2 = C_1$

(ii) Exponential function: $k_2(t) = C_1 \exp(-t/C_2)$

(iii) Hyperbolic function: $k_2(t) = C_1 /(C_2 + t)$

Here, the time-dependent $k_2(t)$ in (ii) and (iii) types means that a part of unstable fine particulate Fe converts to more stable particulate Fe with time. The constant values of C_1 and C_2 were determined by fitting procedure in order to search for best fitting of temporal decrease in the dissolved Fe concentration (D_{Fe}) in the Fe(III) hydrolytic precipitation experiment at 10°C (Fig. 5). The calculated D_{Fe} changes with time, which is the most similar to the measured D_{Fe} change, were given at $C_1 = 1$ d^{-1} in the type (i), (C_1, C_2) = (8 d^{-1}, 2) in the type (ii) and (C_1, C_2) = (5, 1.5 d^{-1}) in the type (iii).

In case of type (i) with constant k_2, the equilibrium state between dissolved Fe and particulate Fe is rapidly performed at an early stage and then the temporal decrease in the dissolved Fe concentration in the Fe(III) hydrolytic precipitation experiment can not be reproduced at all (Fig. 7-(i)). In comparison between types (ii) and (iii) with time-dependent $k_2(t)$, it is found that the calculated D_{Fe} change using hyperbolic function (type (iii)) is much better consistent with the temporal measured D_{Fe} change in the hydrolytic precipitation experiment. It is assumed that a true back reaction rate constant is k_2*, i.e., $C_1 = k_2$* in the types (ii) and (iii) so that temporal change in $k_2(t)$ is due to the chemical conversion process from unstable fine particulate Fe to stable particulate Fe phase. Therefore, the term of $k_2(t)P_{Fe}$ in equation (4) is interpreted by $k_2*[\exp(-t/C_2)P_{Fe}]$ in type (ii) *and* $k_2*[P_{Fe} / (C_2 + t)]$ in type (iii).

First, we consider the differential equation with an exponential solution of $[\exp(-t/C_2)P_{Fe}]$, which is easily inferred as follows:

$$dP_{Fe}/dt = -CP_{Fe} \qquad (5)$$

where P_{Fe} is unstable fine particulate Fe concentration and C is constant. This equation form implies that unstable fine particulate Fe converts to stable particulate Fe with a rate constant at any time and continuously decrease. In other words, all of unstable fine particulate Fe finally converts to stable particulate Fe and the equilibrium state between dissolved Fe and particulate Fe is never performed (Fig. 7-(ii)). On the other hand, the differential equation with a hyperbolic solution of $[P_{Fe} / (C_2 + t)]$ is that temporal decrease in P_{Fe} is proportional to the square of P_{Fe} as follows:

$$dP_{Fe}/dt = -CP_{Fe}^{2} \quad (6)$$

This equation can infer an interesting conversion process from unstable fine particulate Fe with large surface area to stable particulate Fe phase (Pankow 1991) such that stable particulate Fe rapidly grow at high P_{Fe} and its growth is slow with decreasing P_{Fe}. Therefore, a small amount of unstable fine particulate Fe can remain for a long time and the equilibrium concentration of dissolved Fe with stable particulate Fe will be performed (Fig. 7-(iii)). Mayer (1982) and Hunter and Leonard (1988) have presented theoretical grounds for expecting second-order particle number kinetics from Brownian aggregation to translate into pseudo-second order removal of riverine dissolved iron (<0.5 μm) after mixing with seawater, remarkably consistent with second-order kinetics with respect to the unstable fine particulate Fe concentration [removal of dissolved iron (<0.025 μm)] in seawater [Eqn. (6)] in the present study. In estuarine mixing system, the fresh iron precipitates with higher bioavailability would be formed through the dissociative hydrolytic precipitation of natural dissolved organic Fe complexes, such as fulvic-Fe(III) complex, supplied by riverine input at both high pH and high concentrations of cations in seawater (Stumm & Morgan 1996; Kuma et al. 1999). Additionally, in mesoscale iron fertilization experiments (Martin et al. 1994; Coale et al. 1996; Boyd et al. 2000, 2004; Tsuda et al. 2003), high concentrations of freshly precipitated am-Fe(III) would have been caused by the supply of concentrated acidic Fe(II) solution to HNLC oceanic regions. The fresh iron precipitates would convert to more stable iron precipitates with less bioavailability with time in seawater.

This is the first confirmation that the maximal cell yields and iron uptake rate of phytoplankton are probably controlled by the solubility and the dissolution rate of am-Fe(III), which decrease with increasing aging time even at 10 and 20°C. The iron nutrition by phytoplankton is strongly related to the dissolution of particulate and colloidal Fe. The conversion from unstable fine am-Fe(III) to stable large am-Fe(III) with time is one of the most important processes in changing the supply of bioavailable Fe(III)' to marine phytoplankton in estuarine and coastal waters and in iron fertilization experiments. In addition, our results suggest that the growth rate of phytoplankton is independent of the amount of intracellularly stored Fe, above a critical concentration of intracellular Fe on the growth, and the maximal cell yields are controlled by a critical

concentration.

Acknowledgments. We thank Dr. K. Suzuki (ES, Hokkaido University) for supplying coastal diatom species and for helpful comments. We also are grateful to anonymous reviewers for their constructive and helpful comments on this work. Partial support was provided by Grant-in-Aids for Environmental Research (No. 023039) from the Sumitomo Foundation and Scientific Research (No. 17651001) from the Ministry of Education, Culture, Sports, Science and Technology, Japan.

References

Anderson MA, Morel FMM (1982) The influence of aqueous iron chemistry on the uptake of iron by the coastal diatom *Thalassiosira weissflogii*. Limnol Oceanogr 27:789–813

Archer DE, Johnson KS (2000) A model of the iron cycle in the ocean. Global Biogeochem Cycle 14:269–279

Boyd PW, others (2000) A mesoscale phytoplankton bloom in the polar Southern Ocean stimulated by iron fertilization. Nature 407:695–702

Boyd PW, others (2004) The decline and fate of an iron-induced subarctic phytoplankton bloom. Nature 428:549–553

Campbell PGC (1995) Interactions between trace metals and aquatic organisms: A critique of the free-ion activity model. In: Tessier A, Turner DR (eds) Metal speciation and bioavailability in aquatic systems. Wiley, New York, p 45–102

Chen M, Wang W-X (2001) Bioavailability of natural colloid-bound iron to marine plankton: Influence of colloidal size and aging. Limnol Oceanogr 46:1956–1967

Chen M, Dei RCH, Wang W-X, Guo L (2003) Marine diatom uptake of iron bound with natural colloids of different origins. Mar Chem 81:177–189

Chen M, Wang W-X, Guo L (2004) Phase partitioning and solubility of iron in natural seawater controlled by dissolved organic matter. Global Biogeochem Cycle 18: GB4013, doi:10.1029/2003GB002160269

Coale KH, others (1996) A massive phytoplankton bloom induced by an ecosystem-scale iron fertilization experiment in the equatorial Pacific Ocean. Nature 383:495–501

Croot PL, Johansson M (2000) Determination of iron speciation by cathodic stripping voltammetry in seawater using the competing ligand 2-(2-Thiazolylazo)-*p*-cresol (TAC). Electroanalysis 12:565–576

Crosby SA, Glasson DR, Cuttler AH, Butler I, Turner DR, Whitfield M, Millward GE (1983) Surface area and porosities of Fe(III)- and Fe(II)-derived oxyhydroxides. Envir Sci Technol 17:709–713

Geider RJ, Roche JL (1994) The role of iron in phytoplankton photosynthesis, and the potential for iron-limitation of primary productivity in the sea. Photosynthesis Res 39:275–301

Guillard RRL, Ryther JH (1962) Studies of marine planktonic diatoms. I. *Cyclotella nana* Hustedt and *Detonula confervacea* (Gleve) Gran. Can J Microbiol 8:229–239

Honeyman BD, Santschi PH (1991) Coupling adsorption and particle aggregation: Laboratory studies of "Colloidal Pumping" using 59Fe-labeled hematite. Environ Sci Technol 25:1739–1747

Hudson RJM, Morel FMM (1989) Distinguishing between extra- and intracellular iron in marine phytoplankton. Limnol Oceanogr 34:1113–1120

Hudson RJM, Morel FMM (1990) Iron transport in marine phytoplankton: kinetics of cellular and medium coordination reactions. Limnol Oceanogr 35:1002–1020

Hudson RJM, Covault DT, Morel FMM (1992) Investigations of iron coordination and redox reactions in seawater using ^{59}Fe radiometry and ion-pair solvent extraction of amphiphilic iron complexes. Mar Chem 38:209–235

Hunter KA, Leonard MW (1988) Colloid stability and aggregation in estuaries: 1. Aggregation kinetics of riverine dissolved iron after mixing with seawater. Geochim Cosmochim Acta 52:1123–1130

Hutchins DA, Franck VM, Brzezinski MA (1999) Inducing phytoplankton iron limitation in iron-replete coastal waters with a strong chelating ligand. Limnol Oceanogr 44:1009–1018

Johnson KS, Gordon RM, Coale KH (1997a) What controls dissolved iron concentrations in the world ocean? Mar Chem 57:137–161

Johnson KS, Gordon RM, Coale KH (1997b) What controls dissolved iron concentrations in the world ocean? Authors' closing comments. Mar Chem 57:181–186

Kuma K, Matsunaga K (1995) Availability of colloidal ferric oxides to coastal marine phytoplankton. Mar Biol 122:1–11

Kuma K, Nishioka J, Matsunaga K (1996) Controls on iron(III) hydroxide solubility in seawater: The influence of pH and natural organic chelators. Limnol Oceanogr 41:396–407

Kuma K, Katsumoto A, Kawakami H, Takatori F, Matsunaga K (1998a) Spatial variability of Fe(III) hydroxide solubility in the water column of the northern North Pacific Ocean. Deep-Sea Res I 45:91–113

Kuma K, Katsumoto A, Nishioka J, Matsunaga K (1998b) Size-fractionated iron concentrations and Fe(III) hydroxide solubilities in various coastal waters. Estuar Coast Shelf Sci 47:275–283

Kuma K, Tanaka J, Matsunaga K (1999) Effect of natural and synthetic organic-Fe(III) complexes in an estuarine mixing model on iron uptake and growth of a coastal marine diatom, *Chaetoceros sociale*. Mar Biol 134:761–769

Kuma K, Tanaka J, Matsunaga K, Matsunaga K (2000) Effect of hydroxamate ferrisiderophore complex (ferrichrome) on iron uptake and growth of a coastal marine diatom, *Chaetoceros sociale*. Limnol Oceanogr 45:1235–1244

Kuma K, Isoda Y, Nakabayashi S (2003) Control on dissolved iron concentrations in deep waters in the western North Pacific: iron(III) hydroxide solubility. J Geophys Res 108(C9), 3289, doi:10.1029/2002JC001481

Liu X, Millero FJ (2002) The solubility of iron in seawater. Mar Chem 77:43–54

Maldonado MT, Price NM (1996) Influence of N substrate on Fe requirements of marine centric diatoms. Mar Ecol Prog Ser 141:161–172

Maldonado MT, Price NM (2000) Nitrate regulation of Fe reduction and transport by Fe-limited *Thalassiosira oceanica*. Limnol Oceanogr 45:814–825

Maldonado MT, Price NM (2001) Reduction and transport of organically bound iron by *Thalassiosira oceanica* (Bacillariophyceae). J Phycol 37:298–309

Martin JH, others (1994) Testing the iron hypothesis in ecosystems of the equatorial Pacific Ocean. Nature 371:123–129

Mayer L (1982) Aggregation of colloidal iron during estuarine mixing: Kinetics,

mechanism, and seasonality. Geochim Cosmochim Acta 46: 2527–2535
Morel FMM, Rueter JG, Anderson DM, Guillard RRL (1979) Aquil: A chemically defined phytoplankton culture medium for trace metal studies. J Phycol 15:135–141
Morel FMM, Hering JG (1993) Principles and applications of aquatic chemistry. Wiley-Interscience, New York
Nakabayashi S, Kusakabe M, Kuma K, Kudo I (2001) Vertical distributions of iron(III) hydroxide solubility and dissolved iron in the northwestern North Pacific Ocean. Geophys Res Lett 28:4611–46
Nishioka J, Takeda S (2000) Change in the concentrations of iron in different size fractions during growth of the oceanic diatom *Chaetoceros* sp.: importance of small colloidal iron. Mar Biol 137:231–238
Obata H, Karatani H, Nakayama E (1993) Automated determination of iron in seawater by chelating resin concentration and chemiluminescence detection. Anal Chem 65:1524–1528
Obata H, Karatani H, Matsui M, Nakayama E (1997) Fundamental studies for chemical speciation of iron in seawater with an improved analytical methods. Mar Chem 56:97–106
Pankow JE (1991) Aquatic chemistry concepts. Lewis, New York
Rich HW, Morel FMM (1990) Availability of well-defined iron colloids to the marine diatom *Thalassiosira weissflogii*. Limnol Oceanogr 35:652–662
Rose AL, Waite TD (2004) Kinetics of iron complexation by dissolved natural organic matter in coastal waters. Mar Chem 84:85–103
Rue EL, Bruland KW (1995) Complexation of Fe(III) by natural organic ligands in the central North Pacific as determined by a new competitive ligand equilibration adsorptive cathodic stripping voltammetric method. Mar Chem 50:117–138
Stumm W, Morgan JJ (1996) Aquatic chemistry, 3rd edn. Wiley-Interscience, New York
Sunda WG, Huntsman SA (1995) Iron uptake and growth limitation in oceanic and coastal phytoplankton. Mar Chem 50:189–206
Sunda WG, Huntsman SA (1997) Interrelated influence of iron, light and cell size on marine phytoplankton growth. Nature 390:389–392
Sunda WG (2001) Bioavailability and bioaccumulation of iron in the sea. In: Turner DR, Hunter KA (eds) The biogeochemistry of iron in seawater. Wiley, New

York, p 41–84
Tani H, Nishioka J, Kuma K, Takata H, Yamashita Y, Tanoue E, Midorikawa T (2003) Iron(III) hydroxide solubility and humic-type fluorescent organic matter in the deep water column of the Okhotsk Sea and the northwestern North Pacific Ocean. Deep-Sea Res I 50:1063–1078
Takata H, Kuma K, Iwade S, Yamajyoh Y, Yamaguchi A, Takagi S, Sakaoka K, Yamashita Y, Tanoue E, Midorikawa T, Kimura K, Nishioka J (2004) Spatial variability of iron in the surface water of the northwestern North Pacific Ocean. Mar Chem 86:139–157
Takata H., Kuma K, Iwade S, Isoda Y, Kuroda H, Senjyu T (2005) Comparative vertical distributions of iron in the Japan Sea, the Bering Sea and the western North Pacific Ocean. J Geophys Res 110: C07004, doi:10.1029/2004JC002783
Tovar-Sanchez A., Sanud0-Wilhemy SA, Garcia-Vargas M, Weaver RS, Popels LC, Hutchins DA (2003) A trace metal clean reagent to remove surface-bound iron from marine phytoplankton. Mar Chem 82:91–99
Tsuda A, others (2003) A mesoscale iron enrichment in the Western subarctic Pacific induces a large centric diatom bloom. Science 300:958–961
Waite TD (2001) Thermodynamics of the iron system in seawater. In: Turner DR, Hunter KA (eds) The biogeochemistry of iron in seawater. Wiley, New York, p 291–342
Wang W-X, Dei RCH (2003) Bioavailability of iron complexed with organic colloids to the cyanobacteria *Synechococcus* and *Trichodesmium*. Aquat Microb Ecol 33:247–259
Weinberg ED (1989) Cellular regulation of iron assimilation. Q Rev Biol 64: 261–290
Wells ML, Zorkin NG, Lewis AG (1983) The role of colloid chemistry in providing a source of iron to phytoplankton. J Mar Res 41:731–746
Wells ML, Mayer LM, Guillard RRL (1991) A chemical method for estimating the availability of iron to phytoplankton in seawater. Mar Chem 33:23–40
Wells ML, Price NM, Bruland KW (1994) Iron limitation and the cyanobacterium *Synechococcus* in equatorial Pacific waters. Limnol Oceanogr 39:1481–1486
Wells ML (1999) Manipulating iron availability in nearshore waters. Limnol Oceanogr 44:1002–1008
Wells ML, Trick CG (2004) Controlling iron availability to phytoplankton in iron-

replete coastal waters. Mar Chem 86:1–13
Wu J, Boyle E, Sunda WG, Wen L-S (2001) Soluble and colloidal iron in the oligotrophic North Atlantic and North Pacifc. Science 293:847–849

Figure captions

Fig. 1. Cell numbers of *C. sociale* at 10°C (a) and *T. weissflogii* at 20°C (b) cultures supplied with direct Fe(III) input and premixed DEB-Fe(III) complex (10:1) with iron concentration of 100 nmol L^{-1}. Data on cell concentrations represent mean (n=3) for triplicate culture experiments.

Fig. 2. Growth of *C. sociale* in direct Fe(III) input medium and solid 1-d, 3-d and 3-w aged am-Fe(III) media (100 nmol Fe L^{-1}, 10°C) and control (without any addition of Fe) without (a) or with (b) addition of DFB after 1 d cultivation. Data on cell concentrations represent mean (n=3) for triplicate culture experiments.

Fig. 3. Growth of *T. weissflogii* in direct Fe(III) input medium and solid 1-d, 3-d and 3-w aged am-Fe(III) media (100 nmol Fe L^{-1}, 20°C) and control (without any addition of Fe) without (a) or with (b) addition of DFB after 1 d cultivation and in direct Fe(III) input and 1-d aged am-Fe(III) media with iron concentration of 10, 25 and 50 nmol L^{-1} at 20°C (20°C). Data on cell concentrations represent mean (n=3) for triplicate culture experiments.

Fig. 4. Long-term iron uptake and growth of *C. sociale* in direct Fe(III) input media and 1-d and 3-d aged am-Fe(III) media without or with addition of DFB after 1 d cultivation. (a) Iron amount accumulated by *C. sociale* in direct Fe(III) input medium and 1-d and 3-d aged am-Fe(III) media with addition of DFB after 1 d cultivation. Each point with ±1 SD at 7.5 d and line are mean cellular iron ([D_{radio}]) for 4 d after addition of DFB. (b) Growth of *C. sociale* in direct Fe(III) input media and 1-d and 3-d aged am-Fe(III) media without or with addition of DFB after 1 d cultivation

Fig. 5. Hydrolytic precipitation rate of Fe^{3+} in seawater with 100 nmol Fe L^{-1} at 10°C

(○) and 20°C (●).

Fig. 6. The daily intracellular Fe per cell in direct Fe(III)-DFB, 1-d aged am-Fe(III)-DFB and 3-d aged am-Fe(III)-DFB media after addition of DFB (dotted line: critical cellular Fe: $[Q_{cri}]= \sim 1x10^{-16}$ mol Fe $cell^{-1}$).

Fig. 7. The hydrolytic precipitation rate models of Fe^{3+} in seawater with 100 nmol Fe L^{-1} at 10°C: (i) Constant value $(k_2 = C_1)$; (ii) Exponential function $[k_2(t) = C_1 exp(-t/C_2)]$; (iii) Hyperbolic function $[k_2(t) = C_1/(C_2 + t)]$ (thick line: hydrolytic precipitation rate model; open circle: observed dissolved Fe concentration).

Fig. 1

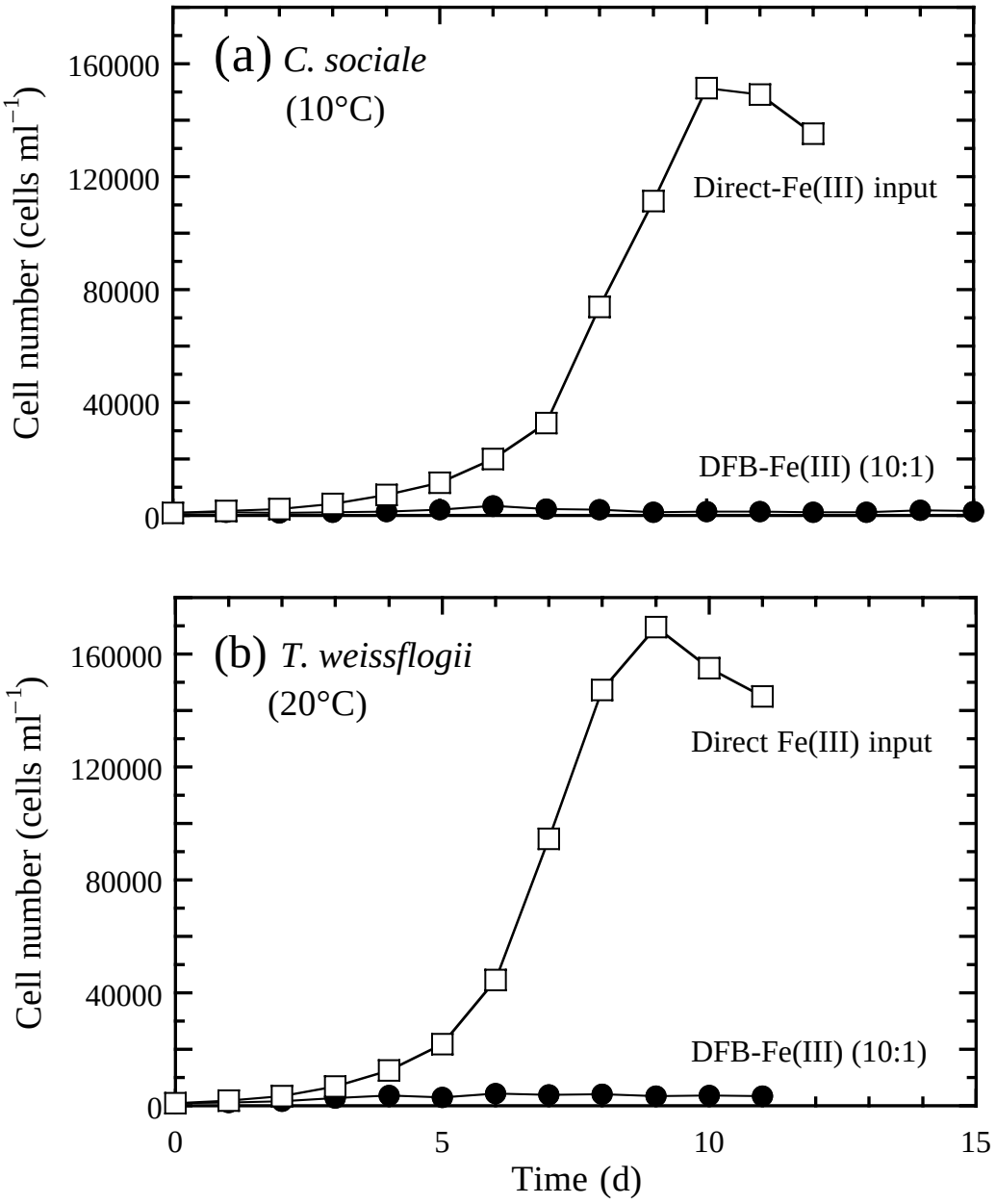
(a) C. sociale
(10°C)
Direct-Fe(III) input
DFB-Fe(III) (10:1)
Cell number (cells ml^{-1})
160000
120000
80000
40000
0
(b) T. weissflogii
(20°C)
Direct Fe(III) input
DFB-Fe(III) (10:1)
Cell number (cells ml^{-1})
160000
120000
80000
40000
0
0
5
10
15
Time (d)

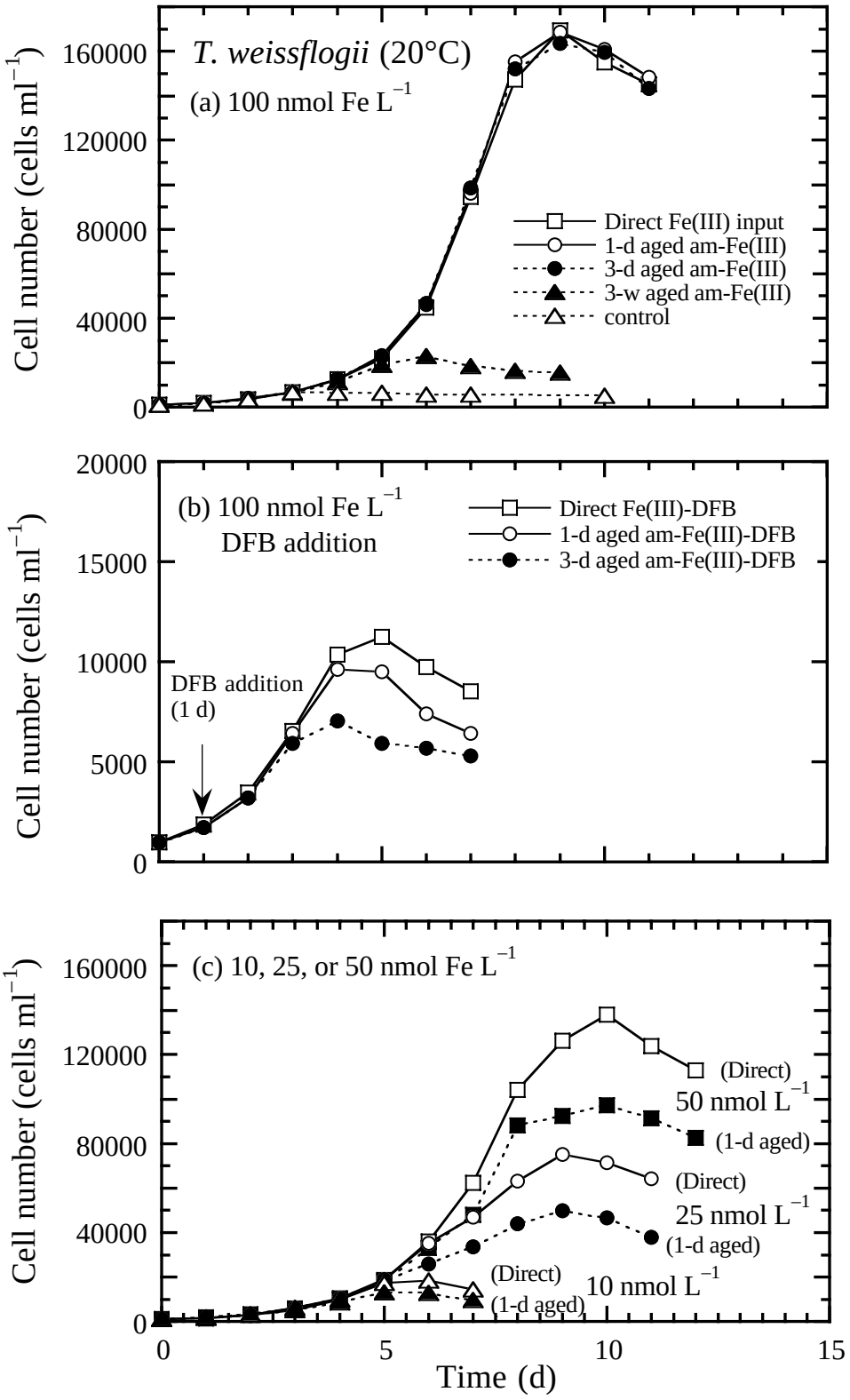
T. weissflogii (20°C)
(a) 100 nmol Fe L−1
Direct Fe(III) input
1-d aged am-Fe(III)
3-d aged am-Fe(III)
3-w aged am-Fe(III)
control
(b) 100 nmol Fe L−1
DFB addition
Direct Fe(III)-DFB
1-d aged am-Fe(III)-DFB
3-d aged am-Fe(III)-DFB
DFB addition
(1 d)
(c) 10, 25, or 50 nmol Fe L−1
(Direct)
50 nmol L−1
(1-d aged)
(Direct)
25 nmol L−1
(1-d aged)
(Direct)
(1-d aged)
10 nmol L−1
Cell number (cells ml−1)
Time (d)

Fig. 2

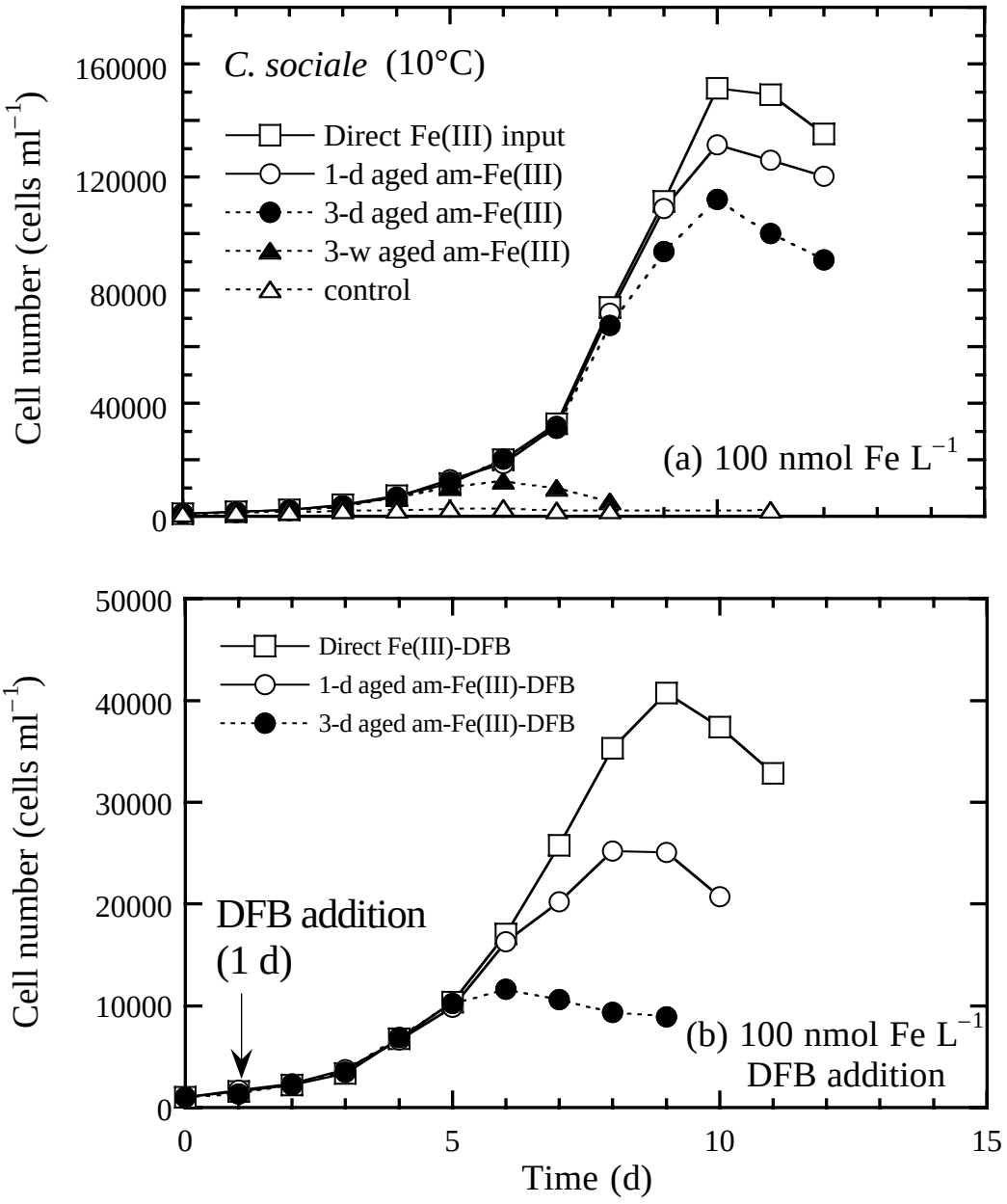
C. sociale (10°C)
Direct Fe(III) input
1-d aged am-Fe(III)
3-d aged am-Fe(III)
3-w aged am-Fe(III)
control
(a) 100 nmol Fe L−1
Cell number (cells ml−1)
160000
120000
80000
40000
0
Direct Fe(III)-DFB
1-d aged am-Fe(III)-DFB
3-d aged am-Fe(III)-DFB
DFB addition
(1 d)
(b) 100 nmol Fe L−1
DFB addition
50000
40000
30000
20000
10000
0
0
5
10
15
Time (d)

Fig. 4

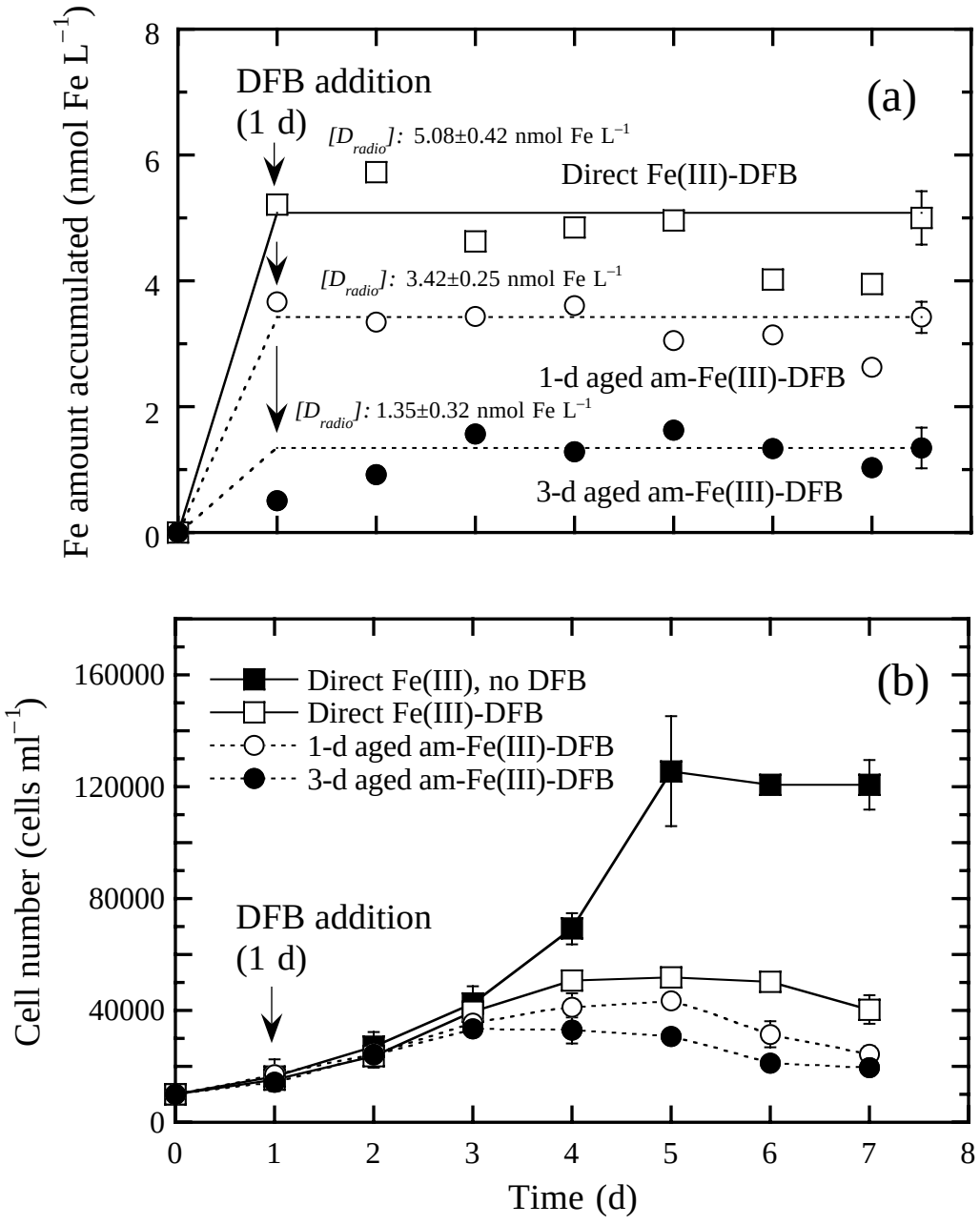
(a)
DFB addition
(1 d)
[D_radio]: 5.08±0.42 nmol Fe L⁻¹
Direct Fe(III)-DFB
[D_radio]: 3.42±0.25 nmol Fe L⁻¹
1-d aged am-Fe(III)-DFB
[D_radio]: 1.35±0.32 nmol Fe L⁻¹
3-d aged am-Fe(III)-DFB
Fe amount accumulated (nmol Fe L⁻¹)
0
2
4
6
8
(b)
Direct Fe(III), no DFB
Direct Fe(III)-DFB
1-d aged am-Fe(III)-DFB
3-d aged am-Fe(III)-DFB
DFB addition
(1 d)
Cell number (cells ml⁻¹)
0
40000
80000
120000
160000
0
1
2
3
4
5
6
7
8
Time (d)

Fig. 5

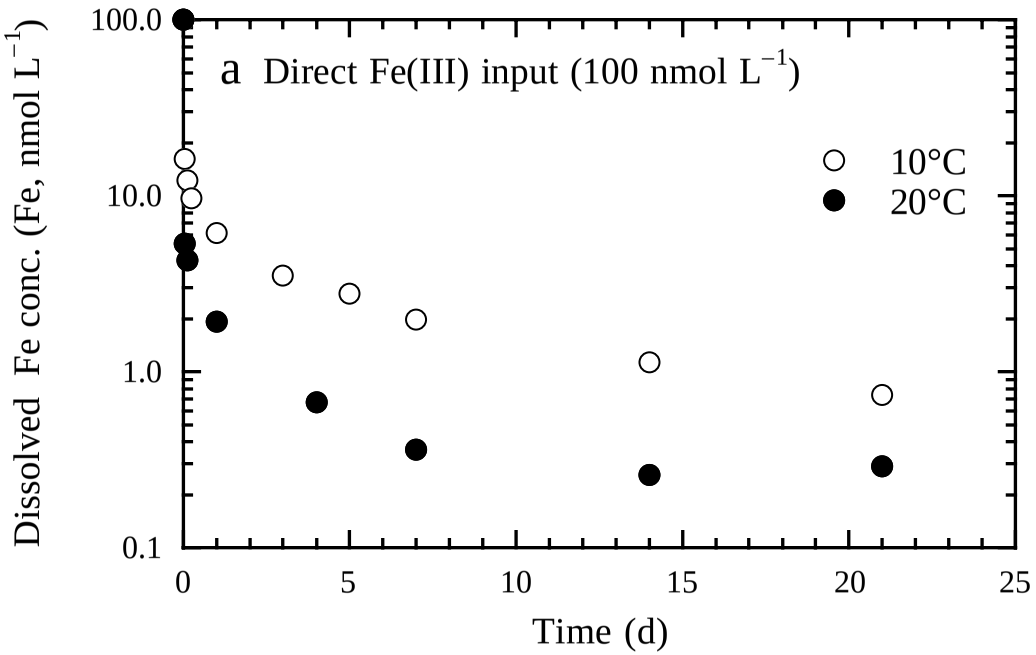
a Direct Fe(III) input (100 nmol L^{-1})
10°C
20°C
Dissolved Fe conc. (Fe, nmol L^{-1})
100.0
10.0
1.0
0.1
0
5
10
15
20
25
Time (d)

Fig. 6

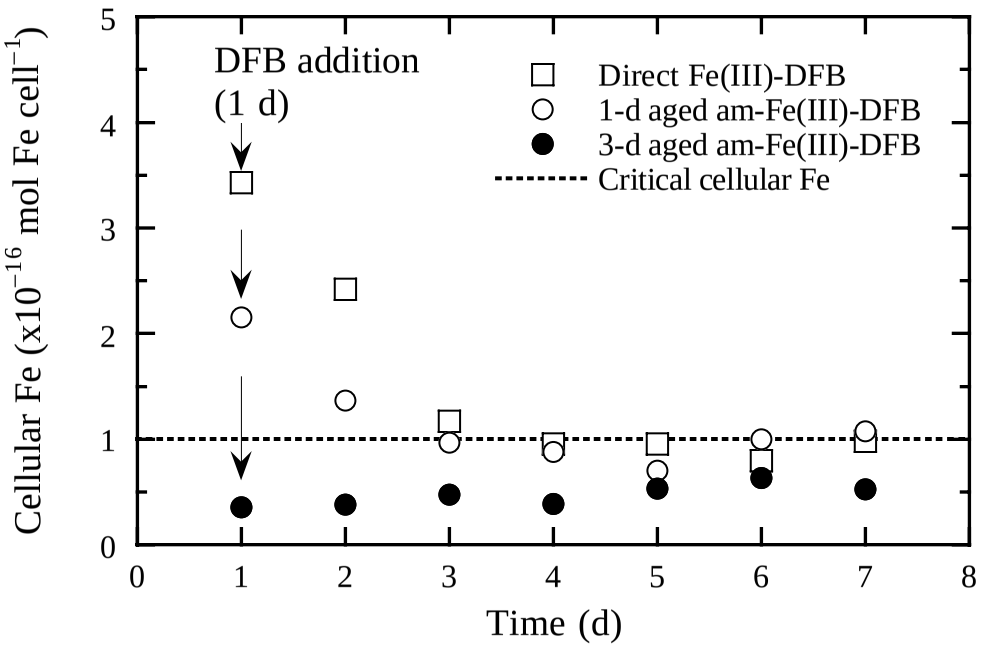
DFB addition
(1 d)
Direct Fe(III)-DFB
1-d aged am-Fe(III)-DFB
3-d aged am-Fe(III)-DFB
Critical cellular Fe
Cellular Fe (x10^{-16} mol Fe cell^{-1})
Time (d)
0
1
2
3
4
5
6
7
8

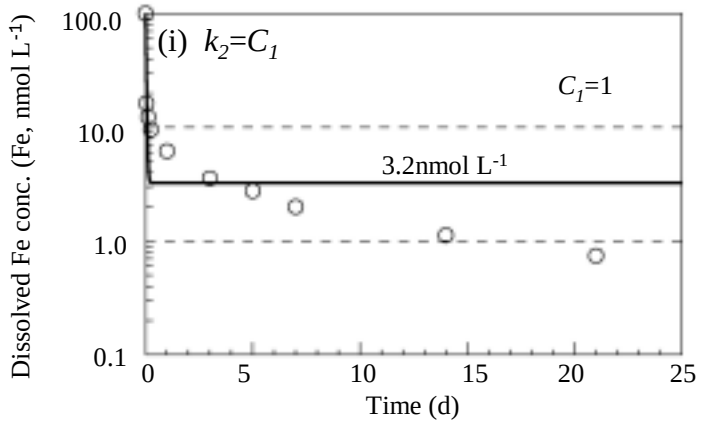
(i) $k_2=C_1$
C_1=1
3.2nmol L^{-1}
Dissolved Fe conc. (Fe, nmol L^{-1})
100.0
10.0
1.0
0.1
0
5
10
15
20
25
Time (d)

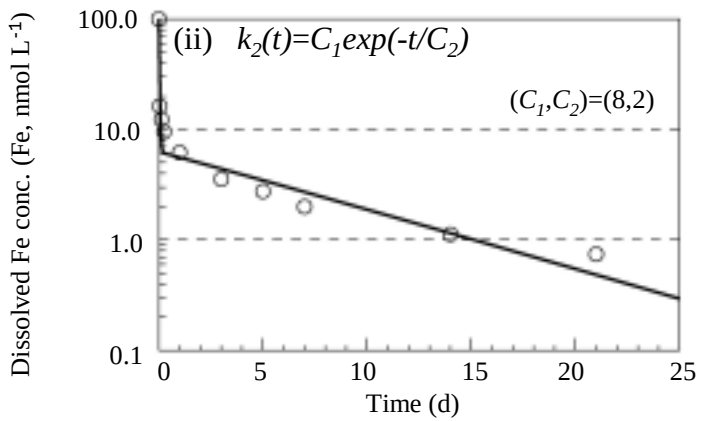
(ii) $k_2(t)=C_1exp(-t/C_2)$
(C_1,C_2)=(8,2)
Dissolved Fe conc. (Fe, nmol L^{-1})
100.0
10.0
1.0
0.1
0
5
10
15
20
25
Time (d)

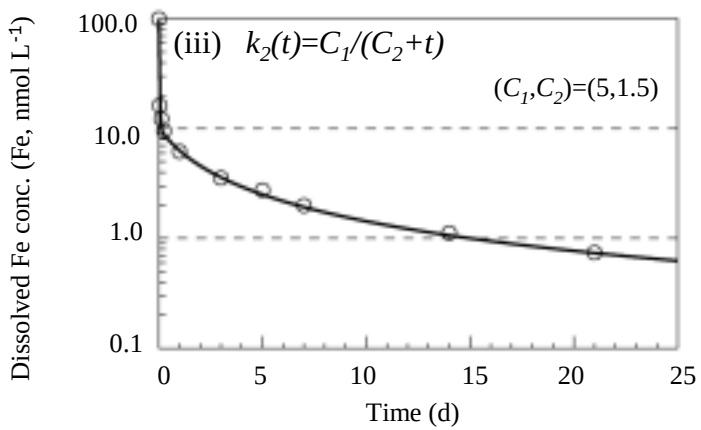
(iii) $k_2(t)=C_1/(C_2+t)$
(C_1,C_2)=(5,1.5)
Dissolved Fe conc. (Fe, nmol L^{-1})
100.0
10.0
1.0
0.1
0
5
10
15
20
25
Time (d)

Table 1. Growth rate and maximal cell yields of *Chaetoceros sociale* (10°C) and *Thalassiosira weissflogii* (20°C) in direct Fe(III) input and 1-d, 3-d and 3-weeks aged am-Fe(III) media which DFB was added after incubation for 1 day or not (Not determined–N). *Values are from our previous study (Iwade *et al.,* submitted).

Medium	Cell number at start (cells ml^{-1})	Addition of DFB ($1\ \mu mol\ l^{-1}$) (DFB : Fe(III) = 10 : 1)	Specific growth rate (μ, d^{-1})	Maximal cell yields [*Cn*] (cells ml^{-1})
			(range for n = 3 or ± 1 SD for n = 1)	
A. *Chaetoceros sociale* (100 nmol L^{-1} Fe concentration, 10°C)				
(1) Growth rate experiment (n = 3, Figs 1a and 2)				
Direct Fe(III) input	1000	no addition	0.51–0.53 (0–10 d)	146,000–155,000
1-d aged am-Fe(III)	1000	no addition	0.52–0.53 (0–9 d)	129,000–133,000
3-d aged am-Fe(III)	1000	no addition	0.50–0.53 (0–7 d)	108,000–117,000
3-w aged am-Fe(III)	1000	no addition	0.45–0.49 (0–5 d)	129,000–133,000
Direct Fe(III) input	1000	DFB (after 1 d incubation)	0.46–0.47 (0–8 d)	39,300–41,100
1-d aged am-Fe(III)	1000	DFB (after 1 d incubation)	0.42–0.47 (0–7 d)	24,400–25,900
3-d aged am-Fe(III)	1000	DFB (after 1 d incubation)	0.42–0.49 (0–5 d)	11,100–12,600
(2) Iron uptake and growth rate experiment (n = 1, Fig. 4)				
Direct Fe(III) input	10000	no addition	*0.50±0.01 (05 d, r=0.999)	*126,000±20,000
Direct Fe(III) input	10000	DFB (after 1 d incubation)	*0.47±0.01 (0–3 d, r=0.999)	*52,000±2,000
1-d aged am-Fe(III)	10000	DFB (after 1 d incubation)	*0.45±0.05 (0–3 d, r=0.994)	*43,000±2,000
3-d aged am-Fe(III)	10000	DFB (after 1 d incubation)	0.44±0.04 (0–3 d, r=0.996)	33.000±1.,000
B–1 *Thalassiosira weissflogii* (100 nmol L^{-1} Fe concentration, 20°C)				
(1) Growth rate experiment (n = 3, Figs 1b, 3a and 3b)				
Direct Fe(III) input	1000	no addition	0.63–0.64 (0–8 d)	169,000–170,000
1-d aged am-Fe(III)	1000	no addition	0.63–0.64 (0–8 d)	160,000–176,000
3-d aged am-Fe(III)	1000	no addition	0.63–0.65 (0–8 d)	157,000–169,000
3-w aged am-Fe(III)	1000	no addition	0.52–0.63 (0–4 d)	21,500–25,600
Direct Fe(III) input	1000	DFB (after 1 d incubation)	0.59–0.60 (0–4 d)	10,700–11,500
1-d aged am-Fe(III)	1000	DFB (after 1 d incubation)	0.57–0.61 (0–4 d)	9,300–10,000
3-d aged am-Fe(III)	1000	DFB (after 1 d incubation)	0.58–0.61 (0–4 d)	6,700–7,400

B–2 *Thalassiosira weissflogii* (10, 25 and 50 nmol L^{-1} concentration, 20°C)

(1) Growth rate experiment (n=3, Fig. 3c)

Direct Fe(III)	(50nM)	1000	no addition	0.59–0.63 (0–8 d)	134,000–140,000
Direct Fe(III)	(25nM)	1000	no addition	0.59–0.61 (0–6 d)	70,400–78,100
Direct Fe(III)	(10nM)	1000	no addition	0.60–0.62 (0–4 d)	18,100–19,300
1-d aged am-	(50nM)	1000	no addition	0.56–0.60 (0–6 d)	93,000–104,000
1-d aged am-	(25nM)	1000	no addition	0.59–0.60 (0–5 d)	47,000–51,900
1-d aged am-	(10nM)	1000	no addition	0.60 (0–2 d)	12,600–13,700

Table 2. Iron uptake by *Chaetoceros sociale* in direct Fe(III) and 1-d and 3-d aged am-Fe(III) media (10°C) which DFB was added after incubation for 1 day. Values of [Q] for the direct Fe(III) input medium and 1-d and 3-d aged am-Fe(III) medium are also the iron uptake rate with unit of mol Fe cell^{-1} d^{-1}. Values of [Q] and [Q_{cri}] in parenthesis were corrected by the percentage of intracellular radiolabelled Fe ([P] in parenthesis). *Values for the 3-d aged am-Fe(III) medium is unreliable because of low iron uptake and incomplete dissolution of aged am-Fe(III) treatment.

Medium	Radiolabelled Fe uptake (for 1 d) [D_{radio}] x10^{-12} mol Fe ml^{-1}	Cell density when DFB was added [C_{DFB}] cells ml^{-1}	Maximal cell yields [Cn] cells ml^{-1}	% of radiolabelled cellular Fe [P] %	Cellular Fe (Fe quota: [Q]) [D_{radio}]/[C_{DFB}]/[P]/100 x10^{-16} mol Fe cell^{-1}	Critical cellular Fe [Q_{cri}] [Q]x[C_{DFB}]/[Cn] x10^{-16} mol Fe cell^{-1}
Iron uptake and growth rate experiment (cell density at start: 10,000, n=1, Fig. 4)						
Direct Fe(III)-DFB	5.08±0.42	15,200±3,400	52,000±1,700	100% (34.2%)	~3.4 (~9.8)	~0.98 (~2.86)
1-d am-Fe(III)-DFB	3.42±0.25	17,000±5,600	43,000±2,200	100% (41.2%)	~2.0 (~4.9)	~0.80 (~1.93)
3-d am-Fe(III)-DFB	1.35±0.32*	14,400±3,300	33,000±1,000	100% (30.6%)	~0.9* (~3.1*)	~0.41* (~1.34*)